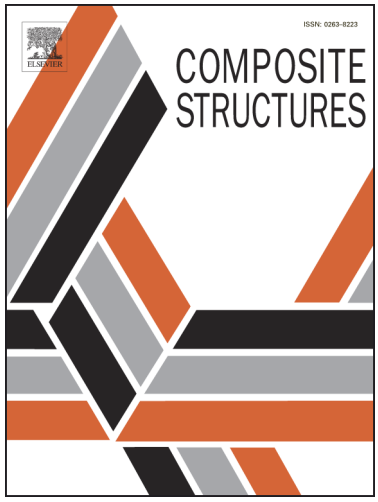

A Novel Thermo-mechanical Anti-icing/De-icing System Using Bi-stable Laminate Composite Structures with Superhydrophobic Surface

Zheng Zhang, BingBin Chen, Congda Lu, Helong Wu, Huaping Wu, Shaofei Jiang, Guozhong Chai

PII: S0263-8223(17)31864-0
DOI: http://dx.doi.org/10.1016/j.compstruct.2017.08.068
Reference: COST 8826

To appear in: *Composite Structures*

Received Date: 14 June 2017
Revised Date: 10 August 2017
Accepted Date: 16 August 2017

Please cite this article as: Zhang, Z., Chen, B., Lu, C., Wu, H., Wu, H., Jiang, S., Chai, G., A Novel Thermo-mechanical Anti-icing/De-icing System Using Bi-stable Laminate Composite Structures with Superhydrophobic Surface, *Composite Structures* (2017), doi: http://dx.doi.org/10.1016/j.compstruct.2017.08.068

A Novel Thermo-mechanical Anti-icing/De-icing System Using Bi-stable Laminate Composite Structures with Superhydrophobic Surface

Zheng Zhang[a*], BingBin Chen[a], Congda Lu[a*], Helong Wu[b], Huaping Wu[a], Shaofei Jiang[a], Guozhong Chai[a]

[a]Key Laboratory of E&M (Zhejiang University of Technology), Ministry of Education & Zhejiang Province, Hangzhou 310014, P.R. China

[b]School of Civil Engineering, The University of Queensland, St Lucia, QLD 4072, Australia

*Corresponding author. E-mail address: zzhangme@zjut.edu.cn (Zheng Zhang), lcd@zjut.edu.cn (Congda Lu). Telephone: 86-571-88320244.

Abstract : A novel anti-icing/de-icing system composed of bi-stable laminate composite structures with superhydrophobic surface and soft electrothermal patch is investigated in this paper. In this system, the superhydrophobic surface has superior performance in anti-icing and de-icing by reducing the adhesion of the ice-skin interface; meanwhile, a thermo-mechanical way to remove ice is conducted by deforming the bi-stable structures using heating actuation method. The superhydrophobic layer is fabricated by decreasing the free energy of copper oxide on the copper surface. The water contact angle of the superhydrophobic surface is tested by an optical contact angle measuring device, which reaches above 155^{o} and the sliding angle is less than 10^{o}. In addition, the microstructure of superhydrophobic layer is characterized by using a scanning electron microscope (SEM) to illustrate the superhydrophobic mechanism. Moreover, outstanding self-cleaning properties and UV-durability are obtained on the prepared surface. Experimental results indicate that the system has good performances in both anti-icing and de-icing processes when working at the subzero temperature. Meanwhile, there is no liquid water left on the surface after the snap-through process of bi-stable structures. Besides, the factors that affect the anti-icing and de-icing performance of system are discussed, including the superhydrophobic property, morphing characteristic of bi-stable laminate composite

structures and actuating method. Finally, the finite element method is used to simulate the factors that affect the deformation of bi-stable structures independently, including the single layer thickness, stacking sequence of the laminate and the embedment of the electrothermal alloy.

Keywords: Anti-icing/de-icing system; Bi-stable laminate composite structures; Superhydrophobic surface; heating actuation method; Finite element method.

1. Introduction

In recent years, the study on the de-icing system has become popular as the ice brings great impacts on energy production [1] and traffic tools, such as wind turbines, aircraft, ship, etc. Many researches have shown that the electrothermal de-icing system based on composite materials is a useful and effective way to remove the ice. For instance, Brian et al. [2] designed a new electrothermal de-icing device for carbon fiber composite aerostructures, which has the ability of anti-icing/de-icing by efficiently transferring electrothermal energy. A self-heating fiber reinforced polymer composite was manufactured by Chu et al. [3] and was tested under the condition of -22^{o}C with the wind speed of 14m/s. The results indicate that the composite materials have a high heat production rate and perform well in the de-icing process.

Although considerable attentions have been given to the composite materials, two aspects are still under discussing: one is how to enhance anti-icing performance without extra energy consummation; another is how to solve the re-freeze problem without continuous heating in low temperature condition when the ice melts. To this end, a new system composed of the bi-stable structures combined with the superhydrophobic surface and soft electrothermal patch is designed in this paper.

The superhydrophobic surface [4] which is originated from the microstructure in natural [5], such as the surface of lotus leaves and rose petals has massive and complex microstructures [6]. It has received considerable attention due to its excellent performances of self-cleaning [7-8], anti-icing [9-10] properties, etc. Various materials can be used as substrate of superhydrophobic surface, including silica gel [11-13], wood [14], graphite [15-16] and metal [17-20]. For instance, Sun et al. [21]

proposed iron-based superhydrophobic surfaces via electric corrosion without bath, and good anti-icing performance was observed in the experiment under condensing conditions. However, most superhydrophobic materials have not integrated with other materials to form new composite structures, which limit the application of superhydrophobic layer. In this paper, the bi-stable structures are integrated with superhydrophobic material so as to form novel bi-stable composite structures.

As to the bi-stable structures, which have two different kinds of stable configurations, can be stable in two shapes without external actuation force [22-23]. Hyer found the bi-stability of unsymmetric composite laminates firstly [24-25]. Then a four-parameter analytical model based on the Rayleigh-Ritz technique was proposed to predict the shapes of bi-stable laminates [26]. Subsequently, researchers have found that the bi-stable structures can be changed from one stable shape to another with external actuations, such as temperature fields [27-29], mechanical forces [30-31], piezoelectric materials [32-33], shape memory alloys [34-36] and electromagnetism [37]. Two main reasons of choosing the bi-stable structures are as following: first, the stable state of bi-stable structures can successfully be transformed through various actuating methods [38], especially the heating method [39]; second, ice protection systems(IPS) consisted of bi-stable structures via a combination of thermal and mechanical mechanisms have been successfully investigated [40-41].

In this paper, an actuating method is used by heating the bi-stable structures locally to achieve the anti-icing and de-icing functions. Moreover, the superhydrophobic surface has been integrated to the bi-stable structures to reduce the adhesion of ice. Therefore, the ice can be shed off by an actuation of the its gravity, vibration or wind [42]. The applications of this anti-icing/de-icing system includes IPS for multifunctional skins and structural members which are exposed to extreme environments, such as wind turbines, bi-stable wing and transport(aerospace) [43].

The schematic diagram of the anti-icing/de-icing system is illustrated in Fig.1, including bi-stable laminate composite structures, superhydrophobic surface and soft electrothermal patch. In this paper, the anti-icing/de-icing system is studied in the next three sections: the fabrication of superhydrophobic surface using the chemical

corrosion method is presented in Section 2 and several characteristic tests are conducted, including water contact angle, microstructure characterization, self-cleaning properties and UV-durability. In addition, the anti-icing and de-icing tests of this new system are conducted under -10°C. Then, the results are given in Section 3 with the discussions of experimental results. In Section 4, the deformation characteristics of bi-stable structures are analyzed to design the bi-stable structures needed for the anti-icing/de-icing system by using the finite element method separately. The effects of the single layer thickness, the stacking sequence, the heating area and the electrothermal alloy are studied respectively.

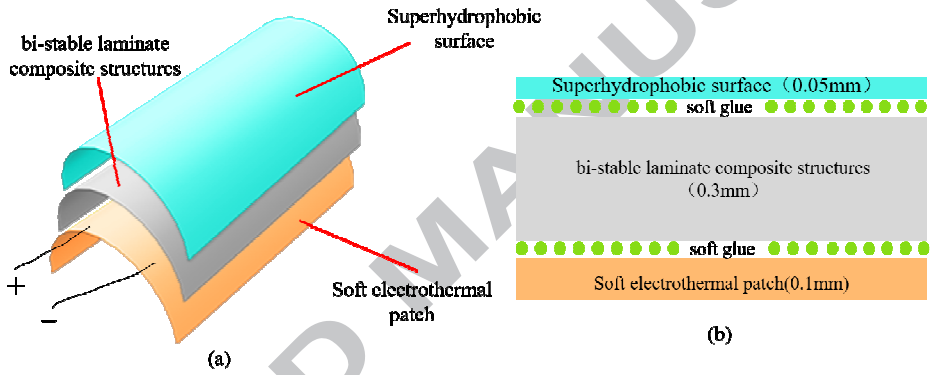

Fig.1. (a)The schematic diagram of the anti-icing/de-icing system; (b)The profile of the anti-icing/de-icing system.

2. Experimental investigation

2.1 Fabrication of superhydrophobic surface

The main materials include deionized water, acetone, anhydrous alcohol, NaOH, H_2SO_4(1mol/L), and $K_2S_2O_8$ (0.064mol/L). These materials are used for preparing the cleaning solution and chemical corrosion solution. Besides, the stearic acid (0.01mol/L) is used for preparing solution that can decrease the free energy of the surface. The substrate is copper foil and the dimension of specimens is 140mm×140mm×0.05mm.

A simple two-steps chemical etching method is used in this paper. Primarily, the nano scale roughness is built in the process of chemical corrosion; then stearic acid

ethanol solution is used to modify the surface energy. The principles of chemical reactions are as follows:

$$K_2S_2O_8+Cu+2KOH \rightarrow 2K_2SO_4+Cu(OH)_2\downarrow \quad (1)$$

$$Cu(OH)_2 \xrightarrow{\Delta} CuO+H_2O \quad (2)$$

More concretely, the preparation of the superhydrophobic surface of the bistable structure surface is as follows: firstly, the copper substrate is bound to the laminate surfaces using soft glue and polished mechanically using 1000# metallographic abrasive papers. Then the acetone, deionized water and anhydrous ethanol are used to remove the oil and impurities from the surface in the ultrasonic condition for 5mins, respectively. In the next step, the copper foil is put into dilute sulfuric acid solution for 30~60s to remove the existing oxide layer. After soaking in the solution of $K_2S_2O_8$ by water bath and heating for 50min at 60°C and placing in a dry box of 100°C for 40mins, a new copper oxide layer owing nano scale roughness is formed. Then, the specimen is put into stearic acid ethanol solution with a concentration of 0.01mol/L for 30mins [44-45]. Finally, the superhydrophobic surface is obtained after drying the copper foil at 100°C.

2.2 Water contact angle and microstructure characterization of superhydrophobic surface

The screenshots of dynamic contact angle are shown in Fig.2 (a), which indicates that the water contact angle reaches 155°. The water droplet (10μL) in the compression and lifting process changes from sphere to ellipsoid and finally recover to sphere, as shown in Fig.2(b). Therefore, the superhydrophobic surface has a lower adhesive property than the copper foil surface, which means that it is beneficial to droplet to bounce or slid when dropping on the surface and less water will stay and freeze in this area.

In addition, the scanning electron microscope (SEM, type: TESCAN VEGA 3 SBH) is used to observe the microstructure of superhydrophobic surface [46]. The SEM micrograph is shown in Fig.3(a), where the picture is magnified by 20,000 times.

It is indicated that the copper oxide has linear and compact microstructure after chemical etching. The schematic diagram of the superhydrophobic surface is given in Fig.3(b). When the microstructures are filled with stearic acid particles, the surface of copper oxide owns superhydrophobic property.

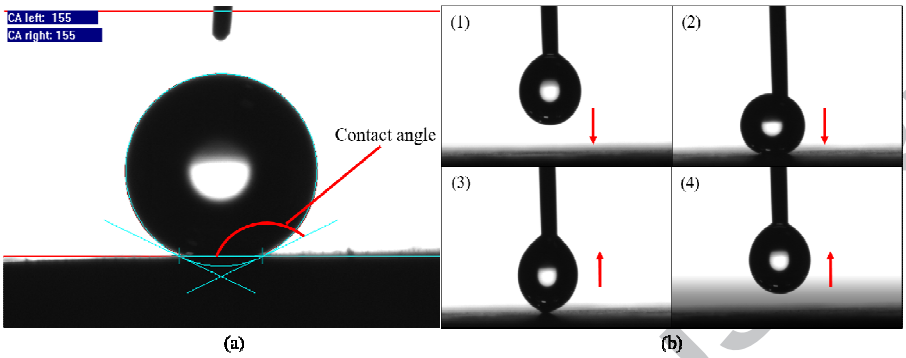

Fig.2. Water contact angle tests of superhydrophobic surface measured by optical contact angle measuring device (Dataphysics OCA30). (a) Static water contact angle. The angle signed with red line is the contact angle between water droplet (10μL) and surface of superhydrophobic surface. (b)Screenshots of dynamic water contact angle. The figures represent the compression and lifting processes of water droplet in the test. Red arrows indicate the moving direction of droplet (10μL).

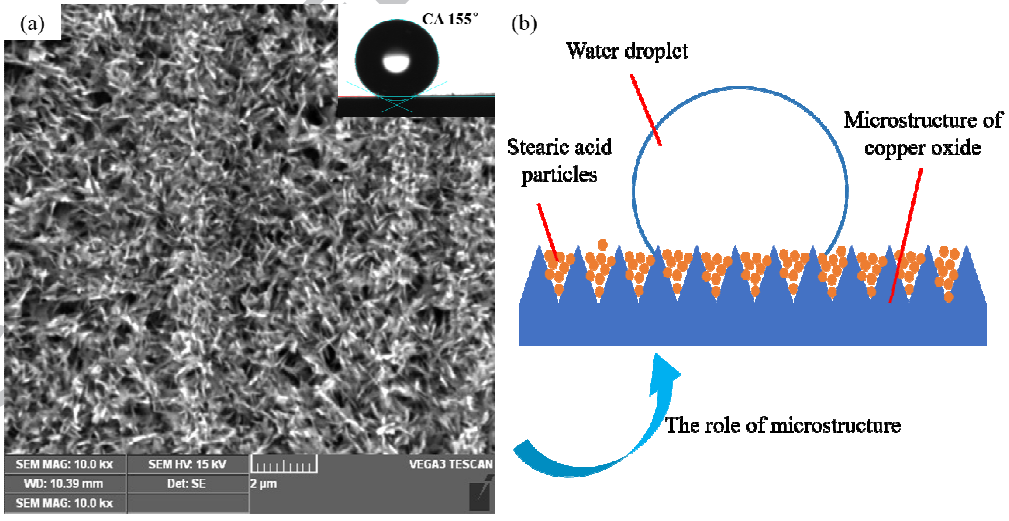

Fig.3. (a) SEM micrographs of copper oxide surface after chemical etching. The surface is magnified by 20,000 times. (b)Schematic diagram of the superhydrophobic surface which is consisted of microstructure of copper oxide and stearic acid particles.

2.3 Self-cleaning properties and UV-durability tests

The self-cleaning is used to prolong the service life of superhydrophobic surface by resisting wear. The self-cleaning function of the superhydrophobic surface is tested with $CaCO_3$ powder as contaminants. In the experiment, the copper foil which has superhydrophobic surface is pasted on the glass slide, and the whole process of self-cleaning test is shown in Fig.4. First, a thin layer of contaminant powders is sprinkled on the superhydrophobic surface and then a water droplet of 0.05ml is placed on the contaminated surface with another on the clean one. As shown in Fig.4(a), the droplets in the two areas remain to be a spherical shape. During the process of sliding, the contaminant powders are immediately adsorbed on the surface of the water droplet and no longer peel off the surface of the water droplet to contaminate the superhydrophobic surface again (Fig.4(b)~4(c)). This phenomenon confirms that the water surface tension is indispensable in adsorbing contaminants. Due to the low surface energy of superhydrophobic surface, the water can carry the contaminants away from the surface.

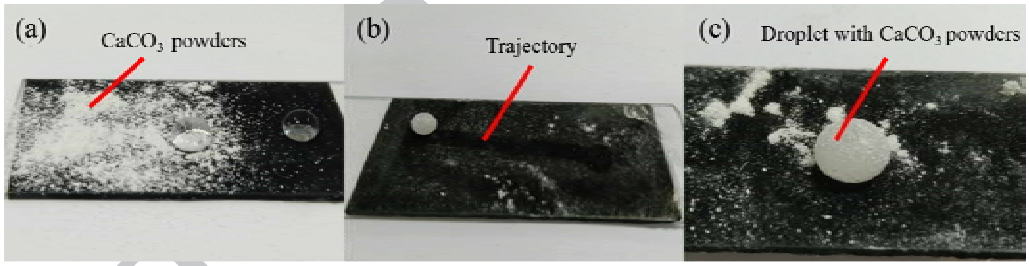

Fig.4. Self-cleaning process on the superhydrophobic surface using deionized water.

LED UV Light Curing System (UP3-314) was used to assess the UV-durability of the superhydrophobic surface. The sample was exposed (the size of exposure area is 2cm×2cm) to UV light(center wavelength: 450nm) for 12h at a room temperature. Besides, the static water contact angle of the sample was measured every 1h. The results are given in Fig.5, which indicates that the sample has the contact angle between 155° and 151° under UV irradiation in different time, suggesting a superior UV-durability. Although the exposure time is not too long, the intensity of UV-light is stronger than that in the sunlight [47].

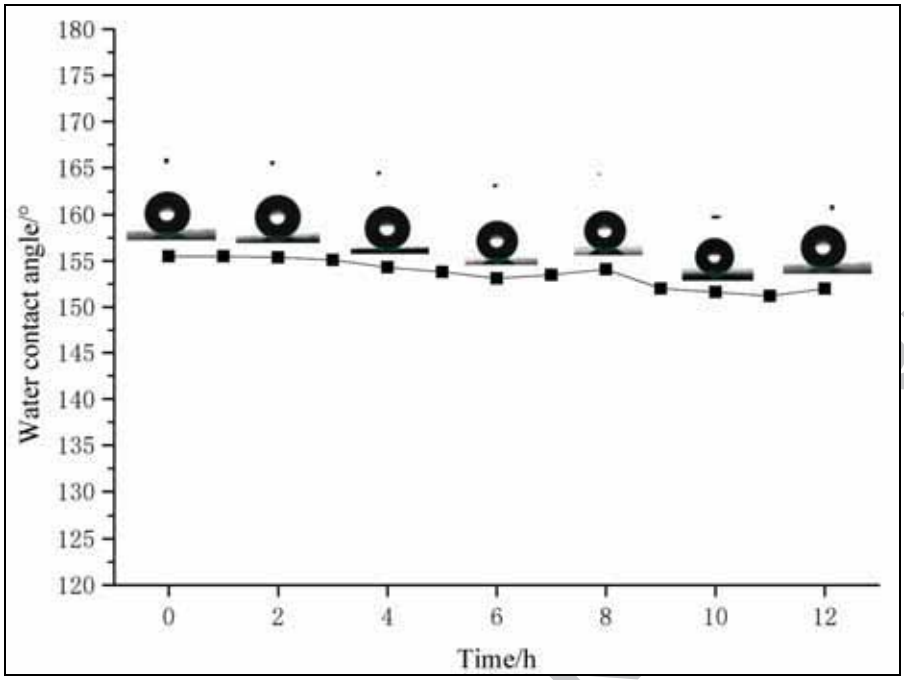

Fig.5 Broken line graph of the CAs of the prepared surface after UV-light exposure. Inset: corresponding optical images of CA.

2.4 Anti-icing tests

The anti-icing test is carried out under -10°C by dripping cold water (which is kept at 0°C) on the surface of bi-stable structures at the rate of 10ml droplets per 10mins for 50mins. In the experiment, two $[0_3/90_3]$ bi-stable laminate composite specimens (140mm×140mm) are used, which are marked as Specimen I and Specimen II, respectively. Specimen I has superhydrophobic surface with a same dimension as the bi-stable structure (140mm×140mm). The results of anti-icing test in Fig.6 indicate that the droplets on the surface remain a spherical shape and few of them are still liquid after 2h; by contrast, Specimen II is covered completely with ice in 1.5h, as shown in Fig.7. Two specimens are weighted fleetly at subzero temperature to compare the quantity of ice left on these two specimens after 3h. The results are shown in Table 1, which indicates that the Specimen I has less ice on the surface using same consumption of water in the same time.

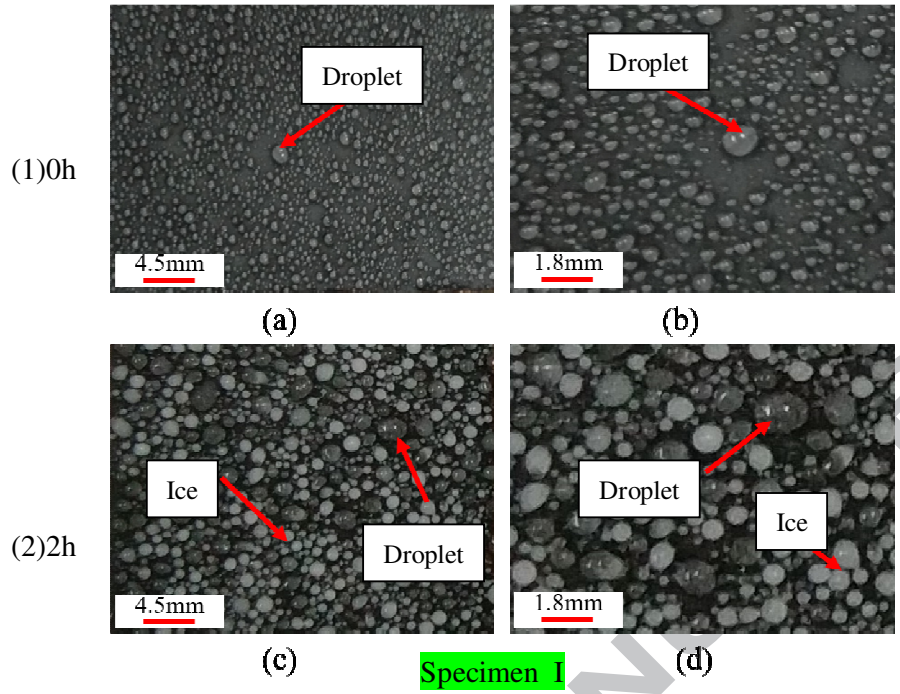

Fig.6 Anti-icing test of Specimen Ⅰ at -10°C. The dimensions of Bi-stable structures and superhydrophobic surface are 140mm×140mm. (b) and (d) are the enlarged views of (a) and (c), respectively

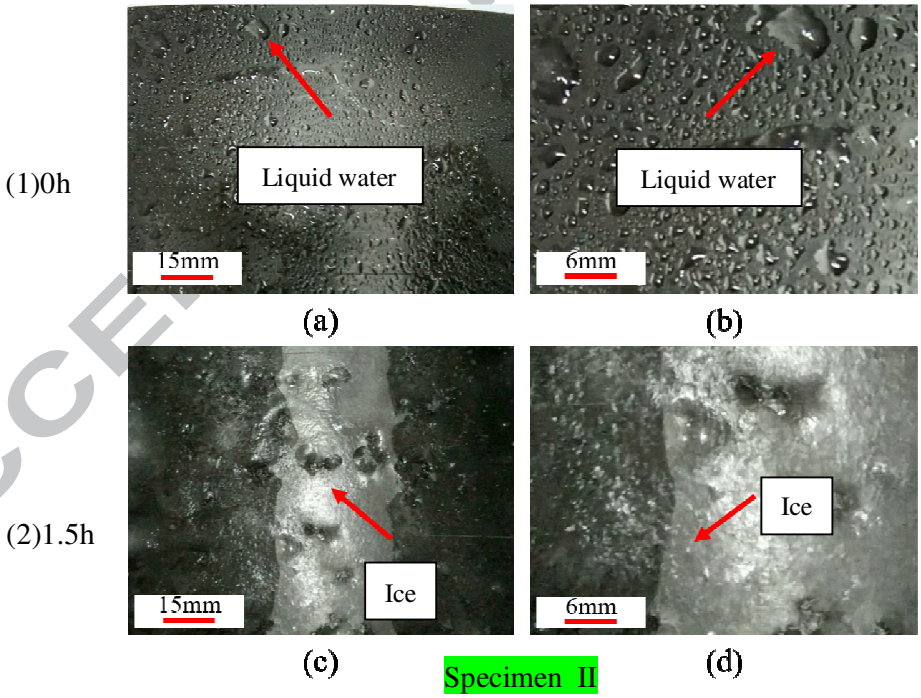

Fig.7. Anti-icing test of Anti-icing test of Specimen Ⅱ at -10°C. The dimensions of Bi-stable structures are 140mm×140mm. (b) and (d) are the enlarged views of (a) and (c), respectively

Table 1. Quality changes of two specimens.

Sample	Initial weight/g	Weight with ice/g	Weight of ice/g
Structures without superhydrophobic surface	4.241	23.993	19.752
Structures with superhydrophobic surface	4.437	17.361	12.924

2.5 De-icing tests

After the anti-icing experiments, more cold water is dripped on the surface of Specimen I to ensure the weight of ice on two specimens same. The soft electrothermal patch (which consists of polyimide and electrothermal alloy) with a power of 25 watts is used in order to melt the ice on the surface and actuate the bi-stable structure. The electrothermal patch is bonded to the surface of bi-stable structures using soft glue and its dimension is 140mm×140mm.

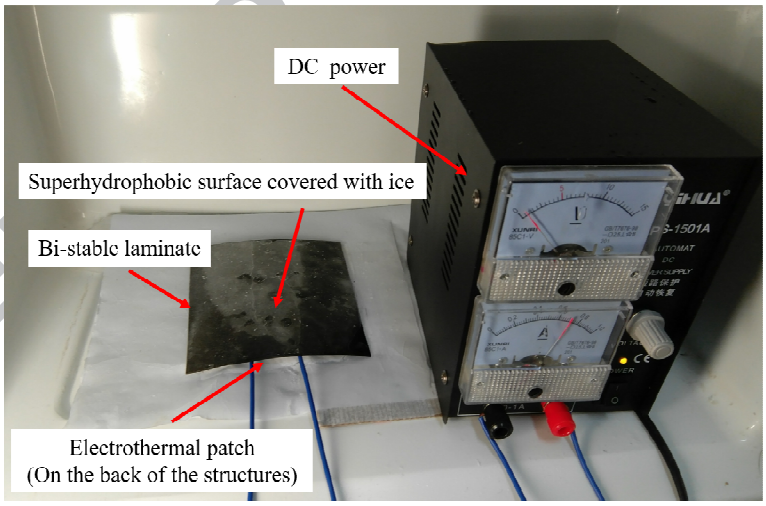

Fig.8. Platform of de-icing experiment. The electrothermal patch is bonded on the back surface of the bi-stable structures which cannot been seen in the figure.

The de-icing experiments are conducted at -10^{o}C in a cool chamber, as illustrated in Fig.8. The results of two specimens in de-icing process are given in Fig.9. As observed, the ice on both two surfaces melts after heating the specimens. Finally,

there is no droplet left on the surface of Specimen I after the snap-through process; by contrast, a spot of water remains on the surface of Specimen II, though the ice on bi-stable structures surface has melted completely.

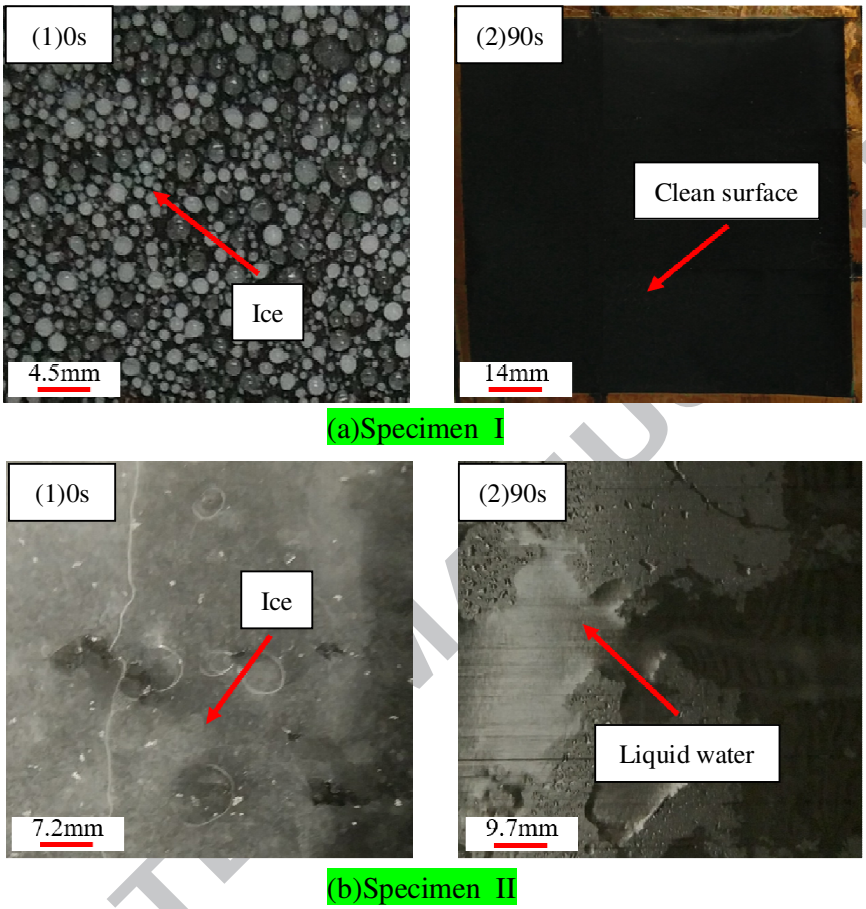

Fig.9. De-icing test of bi-stable structures in low temperature condition (-10^{o}C). The soft electrothermal patches are bonded on the back surface of the bi-stable laminate composite structures. (a)Specimen I is the bi-stable structures with superhydrophobic surface. There is no liquid water on the surface after the de-icing process. (b) Specimen II is the bi-stable structures without superhydrophobic surface. It is obvious that some liquid water still remains on the surface.

3. Discussions of the experimental results

The experimental results in Section 2 indicate that the surface of the system has good superhydrophobic characteristics, self-cleaning performance and UV-durability. Meanwhile, the system performs well in both anti-icing and de-icing processes. Three

main factors of the system have played a positive role, including superhydrophobic surface, bi-stable composite structures and heating method, which will be discussed detailedly in this section.

3.1 The positive influence of superhydrophobic surface

The superhydrophobic surface of the bi-stable structures has a good waterproof property because of its nanostructures and low surface free energy. Fig.6 and in Fig.7 indicate that less droplets can remain on the superhydrophobic surface so that less ice will remain on the surface, as the results shown in Table1. In addition, Fig.6(d) shows that there are still some droplets on the surface when the others have frozen, which demonstrates that the superhydrophobic surface plays an important role in delaying the crystallization of condensed water. In summary, the bi-stable structure integrated with superhydrophobic surface has good anti-icing property without adding extra energy in experiment. As seen in Fig.9, the ice melts completely when heating the bi-stable structures. Then the liquid water slips away from the surface rapidly owning to the superhydrophobic surface in snap-through process. This phenomenon will shorten the period of deicing as well as the heating process, which will reduce the consumption of energy. Besides, the function of self-cleaning will prevent the superhydrophobic surface from wearing due to the dust particles. Above results indicate that the superhydrophobic surface plays an important role in both anti-icing and de-icing processes.

3.2 Effect of the bi-stable composite structures

The bi-stable laminate composite structures made from carbon-epoxy have an excellent thermo-conductive properties and play an important role in transmitting the thermal energy. Moreover, the morphing characteristics of the bi-stable structures cause ice to slid and droplets to bounce away from the surface, as shown in Fig.9(a). Therefore, the ice and droplets can be basically removed to prevent the re-frozen phenomenon without continuously heating the structures. In addition， the configuration of bi-stable structures also affects the anti-icing and de-icing performances of the system. If the curvature radius of the bi-stable structures is too

large, the vibration force produced by snap-through process is not enough to bounce water droplets on the surface; on the other hand, if the curvature radius is too small, the heating temperature will increase with the energy consumption increasing in the meantime. Accordingly, it is greatly important to design the appropriate configuration of bi-stable structures when consider the energy consumption and anti-icing/de-icing performance synthetically. Therefore, finite element analysis method is used to design bi-stable structures, which will be given in Section 4.

3.3 The role of heating method

As the disparity in residual stress between the unheated and heated regions increases, the snap of the whole structure is triggered when the unheated regions lose stability and bend longitudinally. The heating method is quite effective in actuating the bi-stable structures and thawing the ice on the surface. Taking $[0_3/90_3]$ laminates for example, the time of melting ice reduces by 10% and the snap-through temperature decreases by 19.63% when the heating region width increasing from 80mm to 100mm. However, when the heating region width exceeds than 110mm or is smaller than 50mm, the bi-stable structures cannot complete the transition due to the insufficient thermal actuating force of the heated area. In order to minimize the energy consumption of the whole system, an appropriate dimension of the heating area should be selected, which will be discussed in the next section using finite element method.

4. Research on bi-stable characteristics and optimal design of bi-stable composite structures

In this section, the bi-stable characteristics are studied using finite element analysis (FEA) and novel bi-stable composite structures are designed. The discussions in Section 3 indicate that the heating method, the structural characteristics and deformation of the bi-stable structures have great effects on both anti-icing and de-icing processes. Therefore, the FEA method is used to research the factors that affect the bi-stable structures and to design new bi-stable composite structures

[48-49].

The snap-through process is simulated by the finite element method due to the FEA can provide more detailed information [50]. Although the electrothermal patch and the superhydrophobic surface have influence on the bi-stable composite structures, it has little effect on the bi-stable characteristics. Besides, the results of FEA are used to provide references for the deicing experiments and the design of the new composite structures. Consequently, both the electrothermal patch and the superhydrophobic surface are not considered in the FEA.

The bi-stable structures are fabricated by cooling the laminate from the curing temperature to room temperature. Simultaneously, the remaining thermal residual stress after fabrication affects the shape of cross-ply laminates $[0_n/90_n]^T$. Therefore, the snap-through process of bi-stable structures can be achieved by adjusting the local thermal residual stress in FEA or in experiment. In this paper, ABAQUS commercial software (version 6.10) is used to simulate the bi-stable behaviour of such laminate [51]. Four-node shell elements (S4R in ABAQUS) are used, the properties of carbon-epoxy T700/3234 in FEA are listed as follows: the longitudinal modulus E_{11}=123×10^{9}Pa, the transverse modulus E_{22}=8.4×10^{9}Pa, the in-plane shear modulus G_{12}=G_{13}=4.0×10^{9}Pa, the Poisson's ration υ_{12}=0.32, the longitudinal thermal expansion coefficient α_{11}=0.13×10^{-6}/^{o}C, the transverse thermal expansion coefficient α_{22}=43.6×10^{-6}/^{o}C, the thickness of each individual layer t=0.18mm [52].

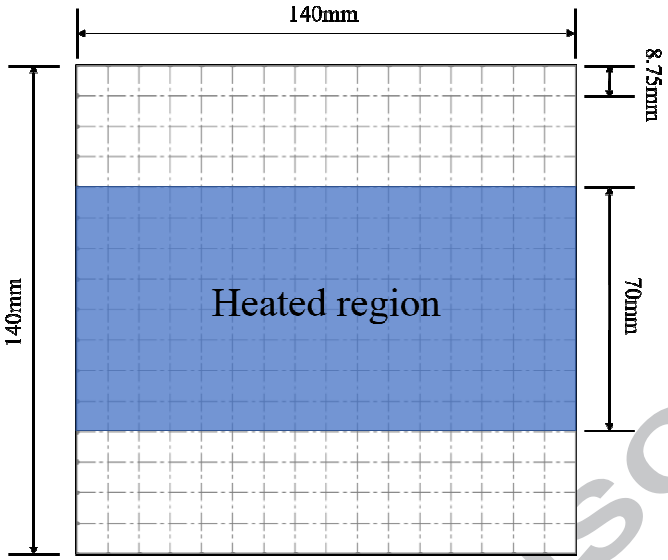

Fig.10. Size of the bi-stable composite laminate model. Blue area is the heated region.

In order to simulate the fabrication process, the bi-stable laminate is clamped consistently at the central point and cooled from curing temperature (180°C, which is maximum temperature in curing process and also the stress-free temperature) to room temperature (20°C) in FEA. Then the model turns to the first stable state. Subsequently, the blue area (as shown in Fig.10) is heated until the structure is transformed, after which the model is cooled down to room temperature again. The whole snap-through processes of the bi-stable structures in FEA are given in Fig.11(a), and the experiment result are given in Fig.11(b). The effects of the thickness of single layer, the stacking sequence, temperature field and electrothermal alloy on snap-through process are discussed below.

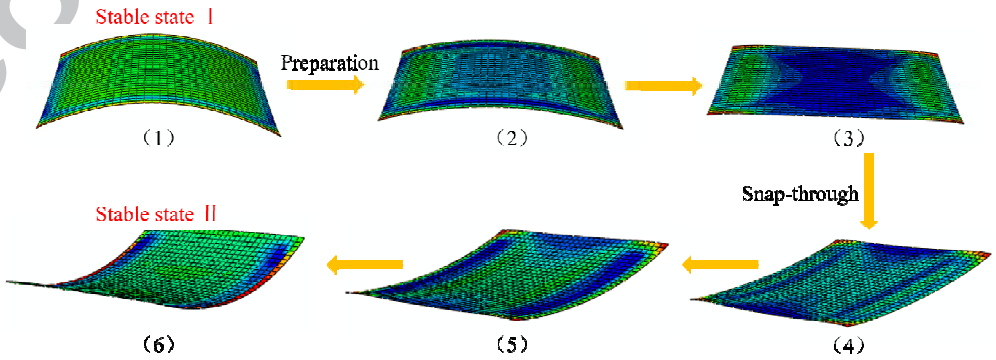

(a)The whole process from fabrication to snap-through of bi-stable structures in FEA.

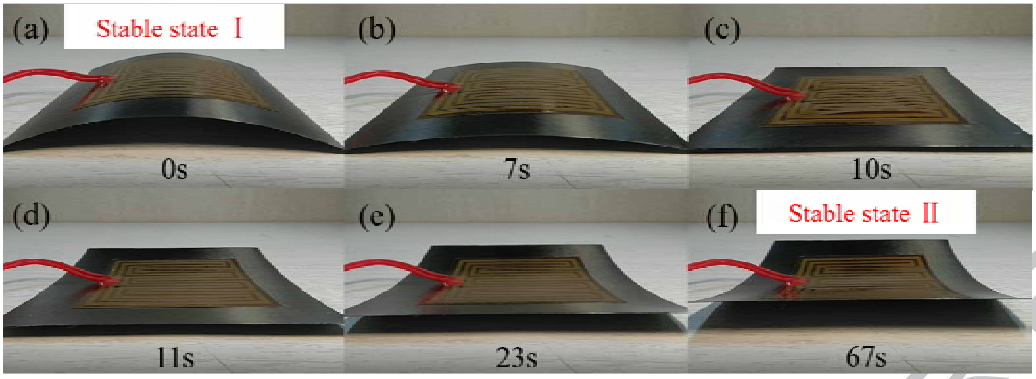

(b) Snap-through process of a $[0_3/90_3]$ laminates in experiment.

Fig.11. Snap-through process of $[0_3/90_3]$ laminates (140mm×140mm) actuated by using heating method.

4.1 Thickness of single layer and the stacking sequence

The predicted curvature radius of $[0_3/90_3]$ laminates and the snap-through temperature with different mesh density in FEA are shown in Fig.12(a) and Fig.12(b), respectively. It shows that with the mesh density increasing, the curvature radius converges to 0.2041m and the snap-through temperature is almost unchanged, which indicates the initial mesh density (meshed by 1024 S4R elements) gives a well-converged solution.

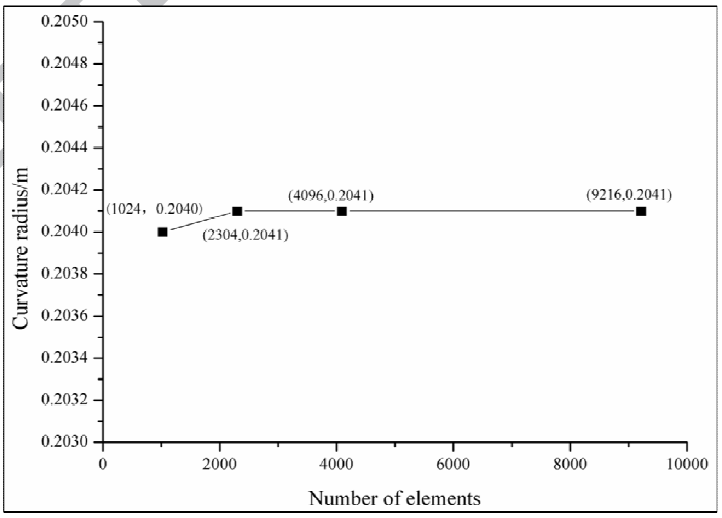

(a)

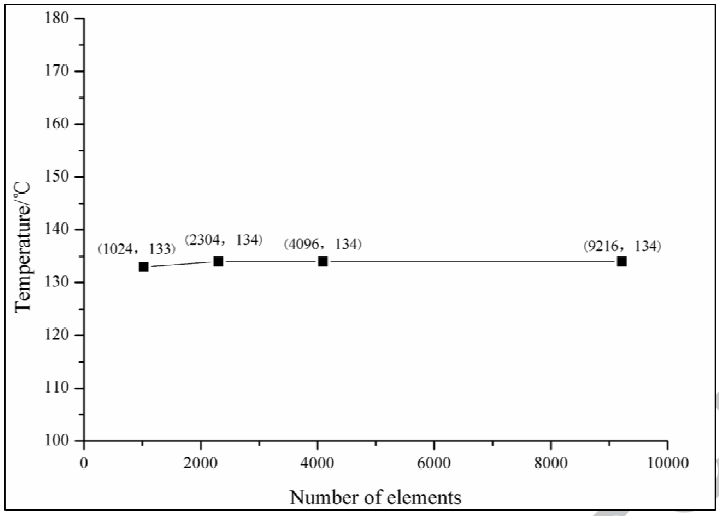

(b)

Fig.12. Influence of mesh density of a $[0_3/90_3]$ laminates on the FEA predicted curvature radius and snap-through temperature.(a) Predicted curvature radius in FEA.(b) Snap-through temperature in FEA.

However, the measured result (0.2193m) is 7.5% larger than that of the FEA result (0.2040m) for the $[0_3/90_3]$ laminates. The main reason of the difference between the experimental and numerical results is the non-linear behaviour in the epoxy matrix material and another may be the existence of resin-rich layer as reported by Panesar et al. [53].

When it comes to the influence of single layer thickness, the predicted curvature radius is shown in Fig.13, and the stacking sequence is also discussed. It is shown that the curvature radius increases with the increasing of the single layer thickness. Meanwhile, the curvature radius of the fabricated bi-stable structures is in good agreement with that of numerical simulation. However, for the $[0_3/90_3]$ laminates, the measured curvature radius is larger and the snap-through temperature is lower than the FEA results. Then the snap-through process of the bi-stable model occurs by applying a local temperature field in FEA, as shown in Fig.14. As to [0/90] and $[0_3/90_3]$ laminates, the temperature of snap-through process decreases with the increasing of single layer thickness. Furthermore, the snap-through temperature of the $[0_3/90_3]$ laminates is much lower than that of the [0/90] laminate.

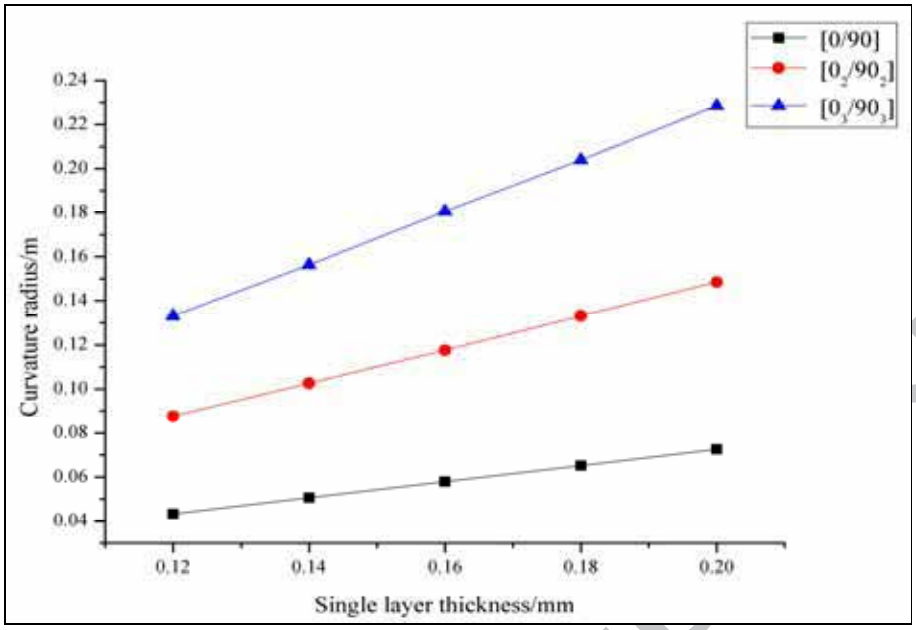

Fig.13. Effect of thickness of single layer on the FEA predicted curvature radius.

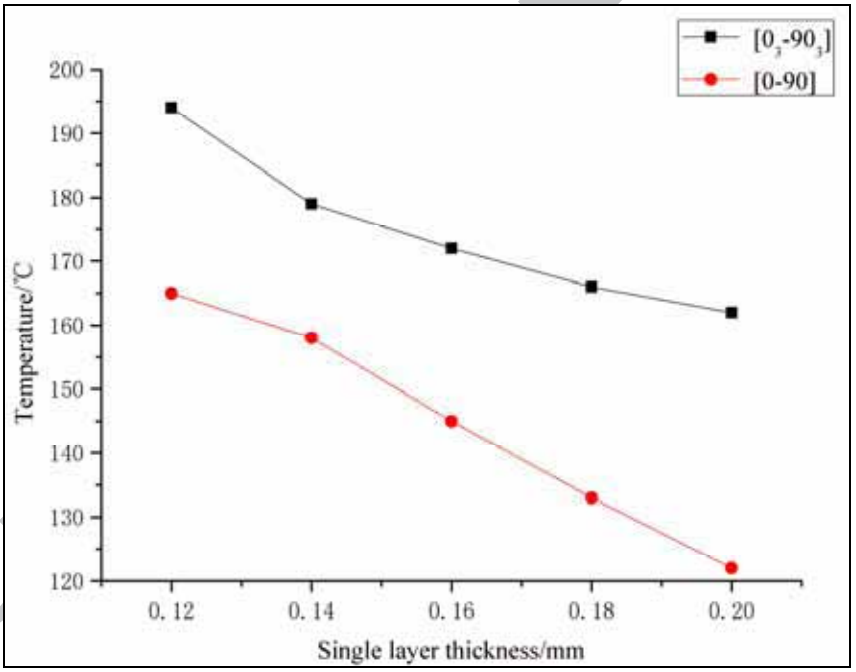

Fig.14. Effect of thickness of single layer on the snap-through temperature in FEA.

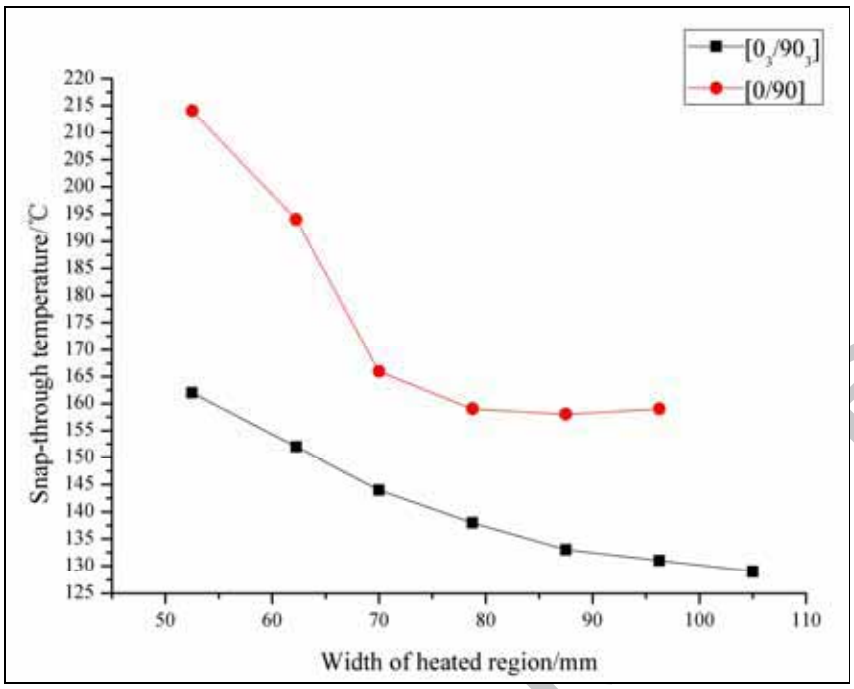

Fig.15. Snap-through temperature vs. width of the heating region of the [0/90] and $[0_3/90_3]$ with same dimensions (140mm×140mm).

4.2 Temperature field

The resulting actuating force depends on the thermal residual stress of the heated region. Thus, the width of the heated region is a significant factor. In FEA, the $[0_3/90_3]$ laminate is studied as an example whose surface is divided into 256 small lattices. As shown in Fig.10, each small lattice has a dimension of 8.75mm×8.75mm. As expected, with the width of the heated region increasing, the temperature of the snap-through process significantly decreases, as given in Fig.15. Nevertheless, when the width of heating region exceeds 105 mm or is smaller than 52.5 mm, the heating actuation method fails. Besides, the results shown in Fig.15 have the same changing trend with those reported by Li [39], though the properties of the bi-stable laminate composite structures are different (CCF300/5438).

The influences of the ice or the mixture of ice and water cannot be neglected, as well as the effect of humidity on material properties [54], which makes the situation complicated in the experiment. According to the results of the de-icing experiments, the time of heating process increases obviously when the surface of bi-stable

structures is frozen by comparing the illustrations in Fig.9 and Fig11(b). But the mixture of ice and water can easily slip from the superhydrophobic surface in snap-through process owning to the superhydrophobic property of the bi-stable structures surface. Therefore, the superhydrophobic layer reduces the energy consumption and makes the system more effective in de-icing process.

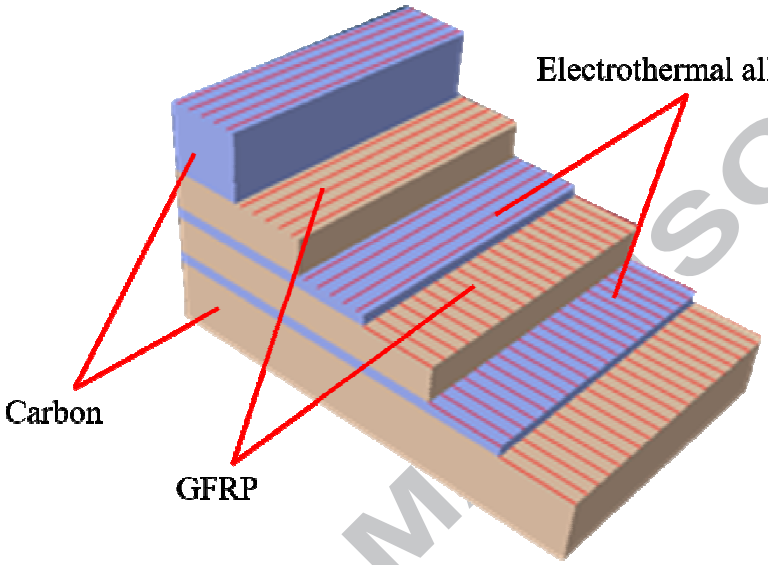

Fig.16. The stacking sequence of the new structures after embedding the electrothermal alloys and GFRP.

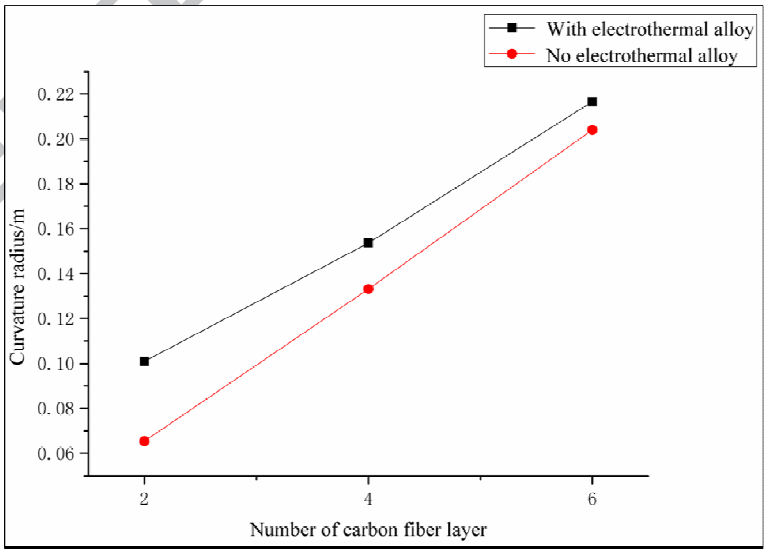

(a)

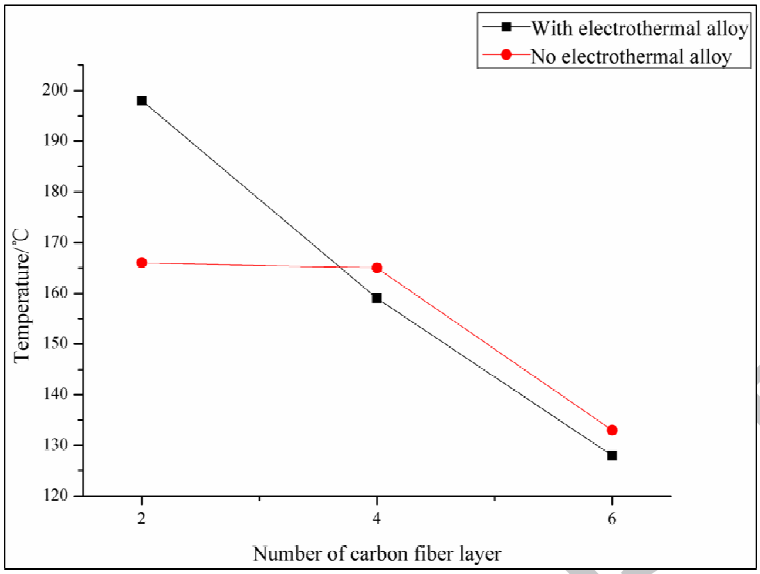

(b)

Fig.17. Influence on the FEA predicted curvature radius and snap-through temperature in FEA after embedding the electrothermal alloys and GFRP. (a)The FEA predicted curvature radius. (b) The snap-through temperature in FEA.

4.3 Electrothermal alloy

In order to reduce the influence of soft electrothermal heating patch, the electrothermal alloy is designed as internal heating sources to actuate the bi-stable structures to change between two stable shapes. A modified FEA model is given in this paper. Firstly, the electrothermal alloys are embedded in the laminates. Besides, the glass fiber-reinforced polymer (GFRP) layers are used to avoid the electric conductive interference between the electrothermal alloys and prepreg. The stacking sequence of the new structures is shown in Fig.16, which has the same dimension (140mm×140mm) as the previous numerical model and the red lines represent the orientation of fibers.

As illustrated in Fig.16, the electrothermal alloys and GFRP are designed to be two layers to keep the characteristic of the original stacking sequences. For example, the [0/ (GFRP, alloy)$_2$/90] laminate is designed to have a similar stacking sequence with the [0/0/90/90] laminates. The results shown in Fig.17(a) indicate that the curvature radius increases compared with the structures without electrothermal alloys

and GFRP. Moreover, it can be seen from Fig.17(b) that the snap-through temperature decreases as the total thickness of the whole structures increases.

5. Conclusions

A novel anti-icing/de-icing system composed of bi-stable laminate composite structures with superhydrophobic surface and soft electrothermal patch is presented in this paper. In this system, the electrothermal patch is used to provide actuating force in snap-through process and transmit the thermal energy. Moreover, the copper foil with superhydrophobic surface is bouded on the surface of the bi-stable structures to enhance the anti-icing/de-icing performance of the system. In the experiment, the ice on the surface of structures is melted completely by heating the bi-stable structures. Simultaneously, with the process of snap-through, little droplets remain on the superhydrophobic surface compared with the region without superhydrophobic surface. The experiment results indicate that: (1) it is a realizable way to achieve de-icing by heating the bi-stable structures using the electrothermal patch. (2) The superhydrophobic layer bonded on the bi-stable structures enhances the water-resistance and anti-icing/de-icing performance of the composite structure system. (3) The new bi-stable composite structures with superhydrophobic surface have superior anti-icing capacity and have excellent performance in de-icing processes when actuated by heating. Further researches on the application of this novel anti/de-icing composite structure system are expected to be done in the next step.

Acknowledgement

This research was supported by the National Natural Science Foundation of China (Grant Nos. 51675485, 11672269), the Zhejiang Provincial Natural Science Foundation of China (Grant No. LY15E050016), the Zhejiang Provincial Public Welfare Technology Application Research Projects (Grant No. 2016C31040).

References

[1] Fakorede O, Feger Z, Ibrahim H, et al. Ice protection systems for wind turbines in cold climate: characteristics, comparisons and analysis[J]. Renewable and Sustainable Energy Reviews, 2016, 65: 662-675.

[2] Falzon B G, Robinson P, Frenz S, et al. Development and evaluation of a novel integrated anti-icing/de-icing technology for carbon fibre composite aerostructures using an electro-conductive textile[J]. Composites Part A: Applied Science and Manufacturing, 2015, 68: 323-335.

[3] Chu H, Zhang Z, Liu Y, et al. Self-heating fiber reinforced polymer composite using meso/macropore carbon nanotube paper and its application in deicing[J]. Carbon, 2014, 66: 154-163.

[4] Schellenberger F, Encinas N, Vollmer D, et al. How water advances on superhydrophobic surfaces[J]. Physical Review Letters, 2016, 116(9): 096101.

[5] Jayaramulu K, Datta K K R, Rösler C, et al. Biomimetic superhydrophobic/superoleophilic highly fluorinated graphene oxide and ZIF‐8 composites for oil–water separation[J]. Angewandte Chemie International Edition, 2016, 55(3): 1178-1182.

[6] Yu H, Liu J, Fan X, et al. Bionic micro-nano-bump-structures with a good self-cleaning property: The growth of ZnO nanoarrays modified by polystyrene spheres[J]. Materials Chemistry and Physics, 2016, 170: 52-61.

[7] Li H, Yu S, Han X. Fabrication of CuO hierarchical flower-like structures with biomimetic superamphiphobic, self-cleaning and corrosion resistance properties[J]. Chemical Engineering Journal, 2016, 283: 1443-1454.

[8] Peng S, Bhushan B. Mechanically durable superoleophobic aluminum surfaces with microstep and nanoreticula hierarchical structure for self-cleaning and anti-smudge properties[J]. Journal of Colloid and Interface Science, 2016, 461: 273-284.

[9] Zheng S, Li C, Fu Q, et al. Development of stable superhydrophobic coatings on aluminum surface for corrosion-resistant, self-cleaning, and anti-icing applications[J]. Materials & Design, 2016, 93: 261-270.

[10]Zigmond J S, Pollack K A, Smedley S, et al. Investigation of intricate, amphiphilic crosslinked hyperbranched fluoropolymers as anti‐icing coatings for extreme environments[J]. Journal of Polymer Science Part A: Polymer Chemistry, 2016, 54(2): 238-244.

[11]Cao M, Guo D, Yu C, et al. Water-repellent properties of superhydrophobic and

lubricant-infused “slippery” surfaces: A brief study on the functions and applications[J]. Applied Materials & Interfaces, 2015, 8(6): 3615-3623.

[12]Li J, Kang R, Tang X, et al. Superhydrophobic meshes that can repel hot water and strong corrosive liquids used for efficient gravity-driven oil/water separation[J]. Nanoscale, 2016, 8(14): 7638-7645.

[13]Mahadik S A, Pedraza F, Vhatkar R S. Silica based superhydrophobic coating for long-term industrial and domestic applications[J]. Journal of Alloys and Compounds, 2016, 663: 487-493.

[14]Tu K, Wang X, Kong L, et al. Fabrication of robust, damage-tolerant superhydrophobic coatings on naturally micro-grooved wood surfaces[J]. Royal Society of Chemistry, 2016, 6(1): 701-707.

[15]Li Z, Tang X Z, Zhu W, et al. Single-step process toward achieving superhydrophobic reduced graphene oxide[J]. Applied Materials & Interfaces, 2016, 8(17): 10985-10994.

[16]Gao X, Zhou J, Du R, et al. Robust superhydrophobic foam: A graphdiyne‐based hierarchical architecture for oil/water separation[J]. Advanced Materials, 2016, 28(1): 168-173.

[17]Chu F, Wu X. Fabrication and condensation characteristics of metallic superhydrophobic surface with hierarchical micro-nano structures[J]. Applied Surface Science, 2016, 371: 322-328.

[18]Guo Z, Chen X, Li J, et al. ZnO/CuO hetero-hierarchical nanotrees array: hydrothermal fabrication and self-cleaning properties[J]. Langmuir, 2011, 27(10): 6193-6200.

[19]Guo J, Yang F, Guo Z. Fabrication of stable and durable superhydrophobic surface on copper substrates for oil–water separation and ice-over delay[J]. Journal of Colloid and Interface Science, 2016, 466: 36-43.

[20]Xu Q F, Wang J N, Sanderson K D. A general approach for superhydrophobic coating with strong adhesion strength[J]. Journal of Materials Chemistry, 2010, 20(28): 5961-5966.

[21]Sun Q, Liu H, Chen T, et al. Facile fabrication of iron-based superhydrophobic surfaces via electric corrosion without bath[J]. Applied Surface Science, 2016, 369: 277-287.

[22]Dano M L, Hyer M W. Thermally-induced deformation behavior of unsymmetric structures[J]. International Journal of Solids and Structures, 1998, 35(17): 2101-2120.

[23]Zhang Z, Wu H, Wu H, et al. Bistable characteristics of irregular anti-symmetric

lay-up composite cylindrical shells[J]. International Journal of Structural Stability and Dynamics, 2013, 13(06): 1350029.

[24]Hyer M W. Some observations on the cured shape of thin unsymmetric structures[J]. Journal of Composite Materials, 1981, 15(2): 175-194.

[25]Hyer M W. Calculations of the Room-Temperature Shapes of Unsymmetric Structurestwo[J]. Journal of Composite Materials, 1981, 15(4): 296-310.

[26]Hyer M W. The room-temperature shapes of four-layer unsymmetric cross-ply structures[J]. Journal of Composite Materials, 1982, 16(4): 318-340.

[27]Li H, Dai F, Du S. The morphing bi-stable glass fiber–reinforced polymer structures actuated by embedded electrothermal alloy[J]. Journal of Intelligent Material Systems and Structures, 2014: 1045389X14521876.

[28]Li H, Dai F, Du S. A morphing bi-stable composite laminate actuated by electric heating method[C]//ASME 2012 Conference on Smart Materials, Adaptive Structures and Intelligent Systems. American Society of Mechanical Engineers, 2012: 53-58.

[29]Zhang Z, Ye G, Wu H, et al. Prediction and Control of the Bi-stable Functionally Graded Composites by Temperature Gradient Field[J]. Materials Science, 2015, 21(4): 543-548.

[30]Cantera M A, Romera J M, Adarraga I, et al. Modelling and testing of the snap-through process of bi-stable cross-ply composites[J]. Composite Structures, 2015, 120: 41-52.

[31]Arrieta A F, Bilgen O, Friswell M I, et al. Passive load alleviation bi-stable morphing concept[J]. Applied Physics Letters, 2012, 111: 07E708.

[32]Masana R, Daqaq M F. Relative performance of a vibratory energy harvester in mono-and bi-stable potentials[J]. Journal of Sound and Vibration, 2011, 330(24): 6036-6052.

[33]Taki M S, Tikani R, Ziaei-Rad S, et al. Dynamic responses of cross-ply bi-stable composite structures with piezoelectric layers[J]. Archive of Applied Mechanics, 2016, 86(6): 1003-1018.

[34]Lee J G, Ryu J, Lee H, et al. Saddle-shaped, bistable morphing panel with shape memory alloy spring actuator[J]. Smart Materials and Structures, 2014, 23(7): 074013.

[35]Henke M, Gerlach G. Mono-and bi-stable planar actuators for stiffness control driven by shape memory alloys[J]. Sensors and Actuators A: Physical, 2016, 238: 95-103.

[36]Barbarion S, Gandhi F S, Visdeloup R. A bi-stable von-mises truss for morphing

applications actuated using shape memory alloys[C]//ASME 2013 Conference on Smart Materials, Adaptive Structures and Intelligent Systems. American Society of Mechanical Engineers, 2013: V001T01A004.

[37]Zhang Z, Wu H, Ye G, et al. Systematic experimental and numerical study of bistable snap processes for anti-symmetric cylindrical shells[J]. Composite Structures, 2014, 112: 368-377.

[38]Bowen C R, Kim H A, Salo A I T. Active composites based on bistable structures[J]. Procedia Engineering, 2014, 75: 140-144.

[39]Li H, Dai F, Du S. Numerical and experimental study on morphing bi-stable composite structures actuated by a heating method[J]. Composites Science and Technology, 2012, 72(14): 1767-1773.

[40]Lee J, Brampton C J, Read J, et al. Investigation of Aligned Conductive Polymer Nanocomposites for Actuation of Bistable Laminates[C]//23rd AIAA/AHS Adaptive Structures Conference. 2015: 1725.

[41]Brampton C J, Pickering S G, Bowen C R, et al. Actuation of Bistable Laminates by Conductive Polymer Nanocomposites for use in Thermal-Mechanical Aerosurface De-icing[C]//55th AIAA/ASME/ASCE/AHS/ASC Structures, Structural Dynamics, and Materials Conference. 2014, American Institute of Aeronautics and Astronautics.

[42]Lv J, Song Y, Jiang L, et al. Bio-inspired strategies for anti-icing[J]. ACS Nano, 2014, 8(4): 3152-3169.

[43]Glover E N K, Bowen C R, Gathercole N, et al. Graphene based skins on thermally responsive composites for deicing applications[C]//SPIE Smart Structures and Materials+ Nondestructive Evaluation and Health Monitoring. International Society for Optics and Photonics, 2017: 101650G-101650G-14.

[44]Zhang Y, Yu X, Zhou Q, et al. Fabrication of superhydrophobic copper surface with ultra-low water roll angle[J]. Applied Surface Science, 2010, 256(6): 1883-1887.

[45]Pei M D, Wang B, Li E, et al. The fabrication of superhydrophobic copper films by a low-pressure-oxidation method[J]. Applied Surface Science, 2010, 256(20): 5824-5827.

[46]Zhang Z, Wu H, He X, et al. The bistable behaviors of carbon-fiber/epoxy anti-symmetric composite shells[J]. Composites Part B: Engineering, 2013, 47: 190-199.

[47]Guo F, Wen Q, Peng Y, et al. Multifunctional hollow superhydrophobic SiO_2 microspheres with robust and self-cleaning and separation of oil/water emulsions

properties[J]. Journal of Colloid and Interface Science, 2017, 494: 54-63.

[48]Giddings P F, Bowen C R, Salo A I T, et al. Bistable composite laminates: effects of laminate composition on cured shape and response to thermal load[J]. Composite Structures, 2010, 92(9): 2220-2225.

[49]Brampton C J, Betts D N, Bowen C R, et al. Sensitivity of bistable laminates to uncertainties in material properties, geometry and environmental conditions[J]. Composite Structures, 2013, 102: 276-286.

[50]Zhang Z, Ye G, Wu H, et al. Thermal effect and active control on bistable behaviour of anti-symmetric composite shells with temperature-dependent properties[J]. Composite Structures, 2015, 124: 263-271.

[51]Zhang Z, Chen D, Wu H, et al. Non-contact magnetic driving bioinspired Venus flytrap robot based on bistable anti-symmetric CFRP structure[J]. Composite Structures, 2016, 135: 17-22.

[52]Zhang Z, Wu H, Ye G, et al. Experimental study on bistable behaviour of anti-symmetric laminated cylindrical shells in thermal environments[J]. Composite Structures, 2016, 144: 24-32.

[53]Panesar A S, Hazra K, Weaver P M. Investigation of thermally induced bistable behaviour for tow-steered structures[J]. Composites Part A: Applied Science and Manufacturing, 2012, 43(6): 926-934.

[54]Brampton C J, Betts D N, Bowen C R, et al. Sensitivity of bistable structures to uncertainties in material properties, geometry and environmental conditions[J]. Composite Structures, 2013, 102: 276-286.